New highly excited states of ^{10}Be observed in charged particle decay

N. R. Fletcher, D. D. Caussyn, and F. Maréchal*
Department of Physics, Florida State University, Tallahassee, Florida 32306-4350, USA

N. Curtis
School of Physics and Astronomy, University of Birmingham, Edgbaston, Birmingham B15 2TT, United Kingdom

J. A. Liendo
Physics Department, Simon Bolivar University, Caracas, Venezuela
(Received 11 March 2003; published 28 August 2003)

Highly excited states of ^{10}Be are formed by the bombardment of ^{7}Li targets by ^{7}Li beams at 34 and 50.9 MeV from the Florida State University Tandem/LINAC accelerator facility. The states are observed in three-body final state reactions by coincidence measurement of the vector momenta of two of the three particles and reconstruction of the decay energies. We observe decays involving ^{7}Li, ^{8}Li, ^{9}Li, and ^{6}He in their ground states, first excited states, and in some cases second excited states. Fifteen of the 18 excitations observed are proposed as possible new states of ^{10}Be. A few α-particle decays of excited boron isotopes are also reported.

DOI: 10.1103/PhysRevC.68.024316 PACS number(s): 25.70.−z, 23.60.+e, 27.20.+n

I. INTRODUCTION

The energy level structure of ^{10}Be is now fairly well understood for excitations below 11.5 MeV. A molecular orbital model [1] seems to provide good correspondence between the calculated excitations and all known excitations up to this energy [2,3], although some predicted unnatural parity states are still missing from the experimental data. The molecular orbital model is a model for the rotational bands, identified by their K^{π} values, of various cluster configurations of two α particles plus two neutrons. Although additional refinement of the calculations might provide better agreement with known excitation energies [3], some recent key measurements [2,4] have provided the connection between known excitations and the characteristics of some of the model states. An α-particle decay branching fraction measurement of the $J^{\pi}=2^{+}$ state at 7.542 MeV, only 132 keV above the α-decay threshold, has identified that state as the $J^{\pi}=2^{+}$ member of the second $K^{\pi}=0_2^{+}$ rotational band. That band, in the model of Itagaki and Okabe [1] has a cluster structure of a ''stretch'' state arrangement, α-2n-α. An α-particle decay angular correlation from the state at $E_x=10.15$ MeV has determined that state to have $J^{\pi}=3^{-}$, identifying that state as the second 3^{-} state of the negative parity K band. The first 3^{-} state of that band is the α particle bound state at $E_x=7.371$ MeV. It had been speculated earlier that the 10.15 MeV state was the first $J^{\pi}=4^{+}$ state [5]. The identification of the 4^{+} states, which have yet to be determined, is essential to the final understanding of the low energy level structure of ^{10}Be.

Our past work on the energy level structure of ^{10}Be has concentrated on the α-particle decays of unbound states [2,4]. Those studies and the present work have used the method of RPDS [6] (resonant particle decay spectroscopy) to investigate three-body final state reactions induced by ^{7}Li+^{7}Li at bombarding energies of 34 and 50.9 MeV by use of the Florida State University Tandem/LINAC accelerator facility. We have also reported decays of ^{10}Be* into ^{7}Li+t near the triton decay threshold [2]. The current work is an extension of the earlier analyses [2,4] to include ^{10}Be* $\rightarrow{}^{9}$Li+p, ^{8}Li+d, ^{7}Li+t, including many decays involving first and second excited states of the lithium isotopes, and the additional high energy decays of ^{10}Be*$\rightarrow{}^{4}$He+^{6}He, ^{4}He +^{6}He*(1.80 MeV). All of these new excited states of ^{10}Be are outside the scope of the current molecular orbital model. The lithium decay channels require breaking one of the α-particle clusters, and the new α decays are from states at higher excitations than have been considered in the model calculations [1,3].

Resonance reactions initiated by ^{7}Li+t have been observed by conventional means [7], however a new $J^{\pi}=0^{-}$ state was found by the current method [2] as a resonance in ^{7}Li*(0.48 MeV)+t. Similarly ^{8}Li+d, ^{9}Li+p, ^{4}He+^{6}He resonances could be observed by use of RIB (rare isotope beam) facilities, but resonances involving excited states of these isotopes still must rely on something similar to RPDS of three-body final state reactions. An exception to this would be resonance reactions such as ^{7}Li$(t,p)^{9}$Li* [8]. This requires simultaneous resonances in ^{10}Be* for both ^{7}Li+t and ^{9}Li*+p, and a resonance can often be masked by the direct reaction nature of the process.

The present work shows that resonances involving rare isotopes and even their excited states can be investigated at conventional beam facilities, and by use of convenient bombarding energies of less than 10 MeV per nucleon. We report many new decay channels for excitations of ^{10}Be from 17 to 28 MeV. All of our charged particle decay work on the energy level structure of ^{10}Be is summarized and compared to other studies of particle unbound states [3,8–13], which have appeared in literature since the 1988 $A=10$ compilation [7]. It is noted that an updated compilation for $A=8,9,10$ is in

*Present Address: IReS, BP 28, F-67037 Strasbourg Cedex 02, France.

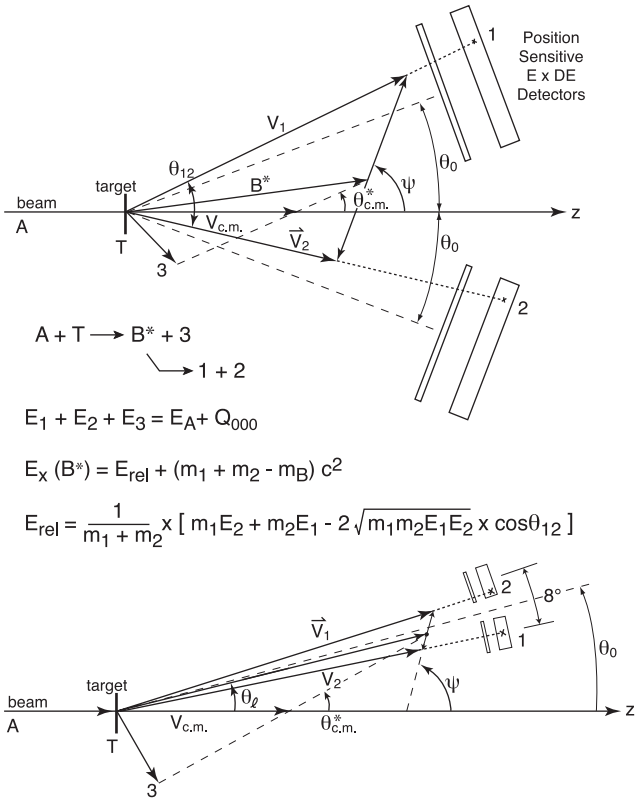

FIG. 1. Velocity addition diagrams for three-body final state reactions, which proceed by sequential two-body decays, equations for the processes, and schematics of detector placements. The wide angle geometry is shown at the top, and the small angle geometry is shown at the bottom.

progress [14]. The recent model calculations [1,15] do not address the excitation energy region of the current experimental results.

II. EXPERIMENTAL METHOD

All of the results reported in this work are the consequences of analysis of data acquired in the previous two experiments [2,4]. The experimental conditions are therefore identical to those already discussed. Detector geometries used and simple forms of the equations used in data reduction are shown in Fig. 1. All detectors used are position-sensitive E-ΔE counter telescopes with position resolutions between 0.5% and 1% of the position-sensitive dimension of the detector. The geometry shown in the upper portion of Fig. 1, the wide angle geometry [4], used detectors 5 cm in length, located $\sim$12 cm from the target, and with $\theta_0 \approx 18.5°$ for ^{7}Li bombarding energy of 34 MeV and $\approx 23°$ for the ^{7}Li bombarding energy of 50.9 MeV. The small angle geometry experiment [2], also at 34 MeV, made use of 12 mm square detectors arranged for x and y position information. These detectors were located $\sim$15 cm from the target and with θ_0 equal to 15°. All isotopes with $A=10$ or less are separated in the counter telescope spectra. The systems therefore provide measurement of A, Z, E, and θ for any charged particle involved in ^{10}Be decay. When two particles are detected in coincidence, their linear momenta allow the determination of the linear momentum of the third particle, when only three particles are involved in the reaction. Construction of an E_{tot} spectrum ($E_{tot}=E_1+E_2+E_3$) then determines the experimental value of the three-body reaction Q value. Q_{000} in Fig. 1 indicates all three particles are in their ground states. The E_{tot} spectra would show lower energy peaks for one or more particles in an excited state.

Figure 1 illustrates what we will call direct detection of the decay, $B^* \rightarrow 1+2$, that is, the decay products of B* are the particles detected in time coincidence. In an important segment of this work, which we call indirect detection, particle 3 is detected in coincidence with either particle 1 or 2, and the reconstructed energy and angle of the undetected decay particle is used to calculate the relative energy between decay particles 1 and 2. The equations shown in Fig. 1 illustrate how the relative energy E_{rel} is determined. The relative energy is of course the decay energy of the state, which when added to the decay threshold energy yields the excitation energy of the unbound state. We have searched the data for charged particle decays of ^{10}Be* involving He and Li isotopes in both direct and indirect detection, and in both the wide angle geometry [4], at bombarding energies of $E_A = 34$ MeV and 50.9 MeV, and the small angle geometry [2], $E_A = 34$ MeV.

III. EXPERIMENTAL RESULTS

A. Direct detection of Li-isotope decays of ^{10}Be

Decays of excited states of ^{10}Be into ^{9,8,7}Li$+p,d,t$ are observed by first selecting the areas from the counter telescope spectra corresponding to the Li isotope of interest and the appropriate $Z=1$ particle. The energy and direction information is used to calculate the energy of the third particle, the E_{tot} spectrum, and ultimately the decay energy E_{rel} and the excitation energy of the ^{10}Be. When an excited state of Li is involved in the decay, it is detected as Li in the ground state following γ decay. The momentum of the emitted γ ray introduces very little spread in the energy and the angle of the emitted Li nucleus and therefore has only a small effect on the subsequently generated spectra. This point is discussed quantitatively in Ref. [2]. Since the γ-ray energy is lost, the value of E_{tot} for events involving an excited state of the lithium isotope is reduced by the γ-ray energy.

1. Wide angle geometry results

For $E_A = 50.9$ MeV, the E_{tot} spectra for three-body final states of ^{9}Li$+p+\alpha$ and ^{8}Li$+d+\alpha$ are shown in Figs. 2(a) and 3(a). The total system energy resolution shown in the E_{tot} spectra is $\approx$800 keV, which is largely influenced by the LINAC resolution. The shaded regions of parts (a) indicate the areas of E_{tot} gated upon to form the excitation spectra in parts (b) and (c), where possible new excitations in ^{10}Be are indicated. Some of the events in these figures can be from the α-particle decay of ^{5}Li and ^{6}Li. These decays can produce some background in the $E_x(^{10}\text{Be})$ spectra, but they cannot produce sharp lines, since the appropriate Dalitz plots are rather oval in shape, unlike those we present later in Sec.

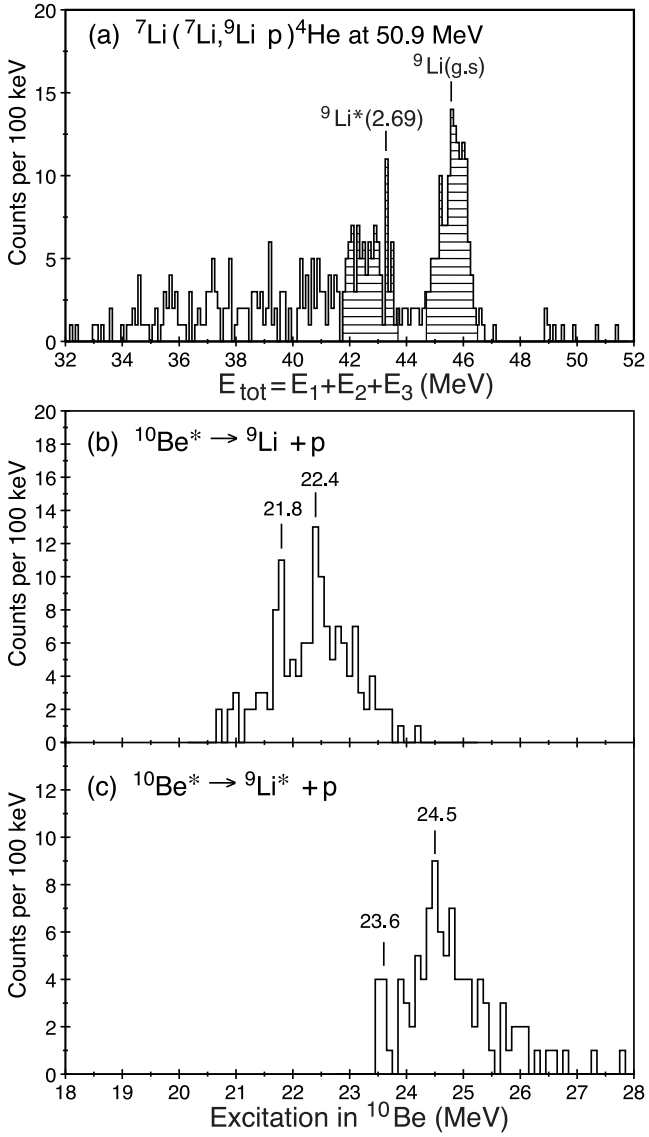

FIG. 2. Direct detection of ^{10}Be* decays using the wide angle geometry, $E_A=50.9$ MeV. (a) E_{tot} spectrum showing shaded gating regions for ^{9}Li(g.s.) and ^{9}Li*(2.69 MeV) decays. (b,c) Spectra of $E_x(^{10}\text{Be})$ for the gating regions shown in (a).

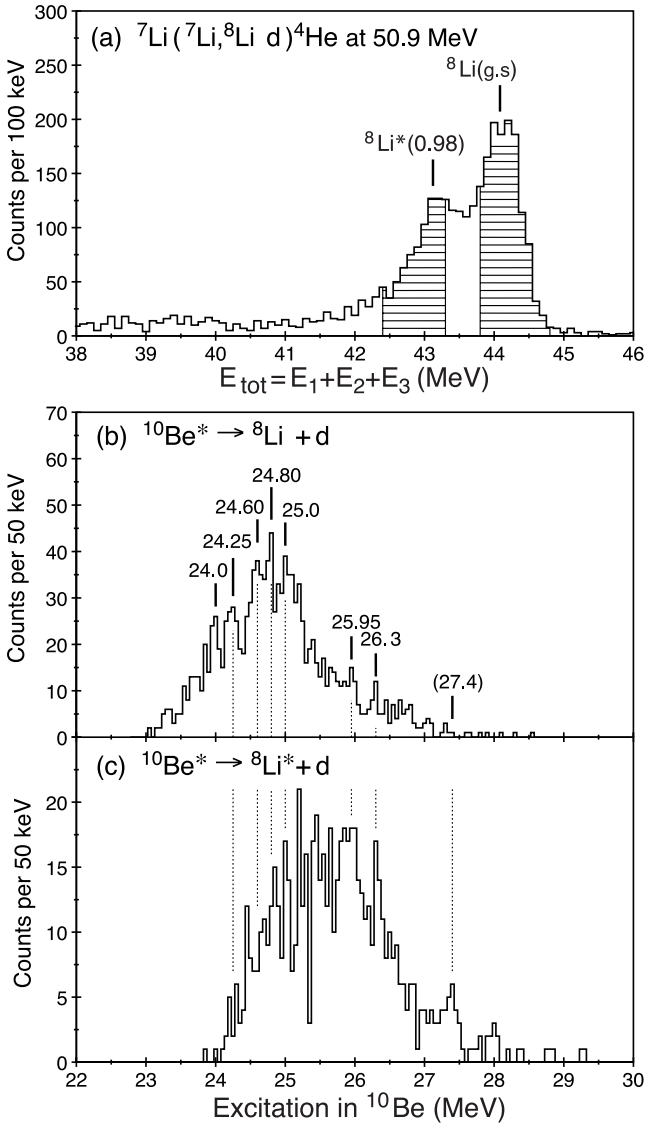

FIG. 3. Direct detection of ^{10}Be* decays using the wide angle geometry, $E_A=50.9$ MeV. (a) E_{tot} spectrum showing shaded gating regions for ^{8}Li(g.s.) and ^{8}Li*(0.98 MeV) decays. (b,c) Spectra of $E_x(^{10}\text{Be})$ for the gating regions shown in (a).

III B 2. With the poor statistical nature of the data of Figs. 2 and 3, it was not useful to try to gate out these possibilities. The shape of the continuum in parts (b) and (c) of these figures tends to indicate the shape of the detection efficiency functions. Examples of these functions have been shown for the direct detection of α decay of ^{10}Be in Fig. 5 in Ref. [2] for the small angle geometry and in Fig. 4 in Ref. [4] for the wide angle geometry. Figures 2(b) and 2(c) show that the accessible energy ranges are only about 3 MeV. This is dictated by the detector geometry and by the kinematics of the method. Since the first excited state of ^{9}Li is at 2.69 MeV, the accessible range in $E_x(^{10}\text{Be})$ is shifted by this amount, thus providing almost no energy overlap in the two excitation spectra of Fig. 2. This lack of overlap frequently prevents comparison of different decay modes of particular excitations. In Figs. 3(b) and 3(c) there is considerable energy overlap, and some of the excitations appear in both spectra (24.8, 25.0, 26.0, and 26.3 MeV) and some do not (24.25, 24.6, and 27.4 MeV). Many possible new excitations of ^{10}Be will be presented, and a summary based on the frequency of occurrence and strength of candidates will determine which are finally considered new states of ^{10}Be.

Direct detection of ^{10}Be decays into $^7\text{Li}+t$ at a bombarding energy of 50.9 MeV is difficult for two reasons. First, since the three-body reaction is $^7\text{Li}+^7\text{Li}\rightarrow^7\text{Li}+t+\alpha$, there is a very large contaminating reaction in which one of the initial state ^{7}Li particles spontaneously breaks up into $t+\alpha$. We can gate out much of this contaminating reaction by forming a Dalitz plot of $E_x(^7\text{Li})$ vs $E_x(^{10}\text{Be})$ for each three-body event analyzed as either reaction. Even after gating out much of the ^{7}Li continuum, considerable background still persists in the $E_x(^{10}\text{Be})$ spectrum. The second difficulty is perhaps more serious. The E_{tot} energy resolution for this part

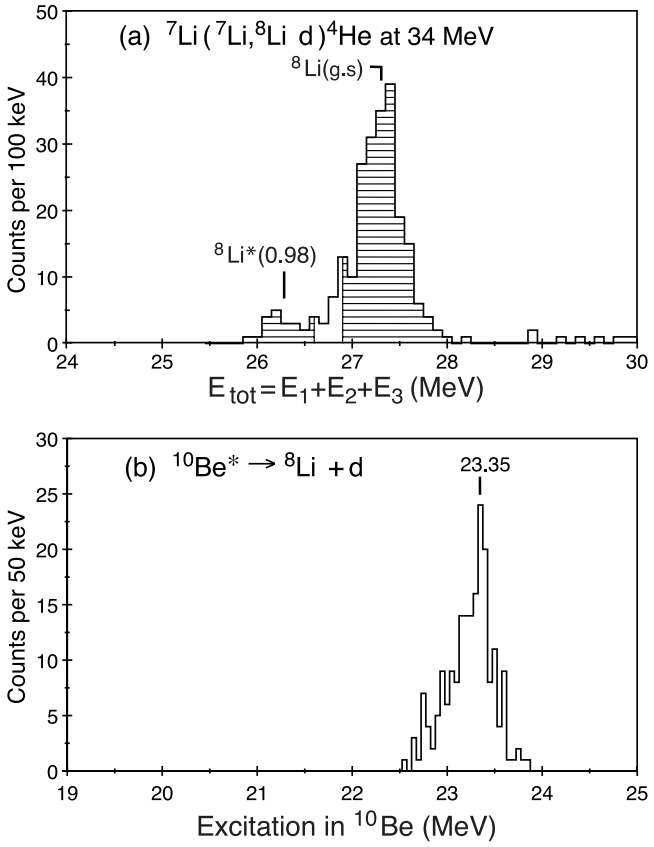

FIG. 4. Direct detection of ^{10}Be* decays using the wide angle geometry, $E_A=34$ MeV. (a) E_{tot} spectrum showing shaded gating regions for ^{8}Li(g.s.) and ^{8}Li*(0.98 MeV) decays. (b) Spectrum of $E_x(^{10}\mathrm{Be})$ for the gating on ^{8}Li(g.s.) region shown in (a).

of the experiment is ≈800 keV, while the separation of the ^{7}Li and ^{7}Li* peaks in this spectrum is only ~480 keV. It is clear from the shape of the E_{tot} spectrum that ground state events occur three to four times more frequently than the excited state events. Gating on the extreme upper end ensures predominantly ground state events, and the resulting $E_x(^{10}\mathrm{Be})$ spectrum identifies excitations at 24.25, 24.0 MeV, and possibly at 23.65 and 23.35 MeV. Trying to extract ^{10}Be excitations from the ^{7}Li* region of the E_{tot} spectrum proved to be much too unreliable.

The energy resolution in the E_{tot} spectrum measured at a bombarding energy of 34 MeV is under 600 keV, making for slightly improved gating for the detection of ^{7}Li (g.s.) and ^{7}Li* (0.48 MeV) events. There are several thousand events in both regions of the spectrum; however, after gating on E_{tot} and reconstructing ^{10}Be* spectra no features indicating identifiable states are found. It appears that spectra are overwhelmingly populated by direct three-body final states of $^7\mathrm{Li}+t+\alpha$ and $^7\mathrm{Li}^*+t+\alpha$ without appreciable presence of sequential binary decay through excited resonant states of either ^{7}Li or ^{10}Be. The decay events $^{10}\mathrm{Be}^*\rightarrow{}^8\mathrm{Li}+d$ were observed with little background and the results are shown in Fig. 4. Excitation in ^{10}Be at 23.35 MeV is supported by the ^{8}Li (g.s.)$+d$ decay spectrum, but nothing of significance results from our analysis of $^8\mathrm{Li}^*+d$ at this bombarding energy. Similarly, ^{10}Be* decays to ^{9}Li (g.s.)$+p$ show a well isolated state at $E_x(^{10}\mathrm{Be})=21.0$ MeV, which is supported by an α decay reported later in this work. There are no results for decays involving excited ^{9}Li.

2. Small angle geometry results

For the small angle geometry experiment at 34 MeV, we have already reported the results for $^7\mathrm{Li}+t$ decays [2]. That result showed energy resolution in E_{tot} of ~400 keV so separation of ^{7}Li ground state and first excited state events was adequate, however, the accessible range of ^{10}Be excitation is only about 1 MeV. For $^8\mathrm{Li}+d$ and $^9\mathrm{Li}+p$ decays the separations in E_{tot} of ground state and excited state decays would be even greater, but no ^{8}Li* or ^{9}Li* decays were observed in this part of the experiment. The number of ground state decays observed is extremely small. Only one event observed in $^8\mathrm{Li}+d$ coincidence occurred at an excitation of 21.7 MeV when analyzed as a ^{10}Be* decay. When analyzed as an indirect detection of a $^6\mathrm{Li}^*\rightarrow\alpha+d$ decay, that one event would indicate a ^{6}Li excitation of 5.54 MeV, which does not correspond to a known state, thus eliminating this process from consideration. There were 11 events for $^9\mathrm{Li}+p$ coincidence. Analyzed as ^{10}Be* decay, nine of the events were well localized at $E_x(^{10}\mathrm{Be})=19.83\pm0.03$ MeV with an estimated width of $\Gamma\sim50$ keV. Although the energy spread observed is much less than the 700 keV expected range of accessibility expected, claiming this peak as a new excitation in ^{10}Be must still be considered uncertain. That excitation is just ~200 keV above the $^9\mathrm{Li}+p$ decay threshold where the small angle detection efficiency is near maximum (see, for example, Fig. 5, in Ref. [2]).

B. Indirect detection of Li-isotope decays of ^{10}Be

1. Wide angle geometry results

In the indirect detection of ^{10}Be decays from $^7\mathrm{Li}+{}^7\mathrm{Li}$ reactions, we measure in coincidence either the $\mathrm{Li}+\alpha$ pair or the $\alpha+(Z=1)$ pair. In general the wide angle geometry is better suited for direct detection decays rather than the indirect detection, a conclusion which will be substantiated below. For the 50.9-MeV data the energy resolution in E_{tot} spectra is often nearly 1 MeV for $\alpha+\mathrm{Li}$ coincidences and less than 600 keV for $\alpha+(Z=1$ particle) coincidences. In spite of the poor energy resolution for $\alpha+\mathrm{Li}$ coincidences, ^{9}Li and ^{8}Li are still adequately resolved from their first excited states for gating purposes, and high and low energy regions of the E_{tot} spectrum for $\alpha+{}^7\mathrm{Li}$ can be used. Reconstructed ^{10}Be spectra from E_{tot} gates on the ^{9}Li (g.s.) region indicate ^{10}Be excitations at 32.4, 34.0, and 35.0 MeV, however, without verification from other spectra we do not include these as new excitiations in our summations. No useful ^{10}Be excitation information is obtained for any other gates on E_{tot} spectra for $\alpha+\mathrm{Li}$ coincidences. The useful information from these coincidence data are for the direct detection of the competing decays of boron isotopes, $^{13,12,11}\mathrm{B}\rightarrow{}^{9,8,7}\mathrm{Li}\ (\mathrm{g.s.})+\alpha$. Excitation energy spectra for the α decay of boron isotopes are shown in Fig. 5. Only unambiguous strong decays are labeled. The new state in ^{13}B at $E_x=13.6$ MeV may be accompanied by several higher energy

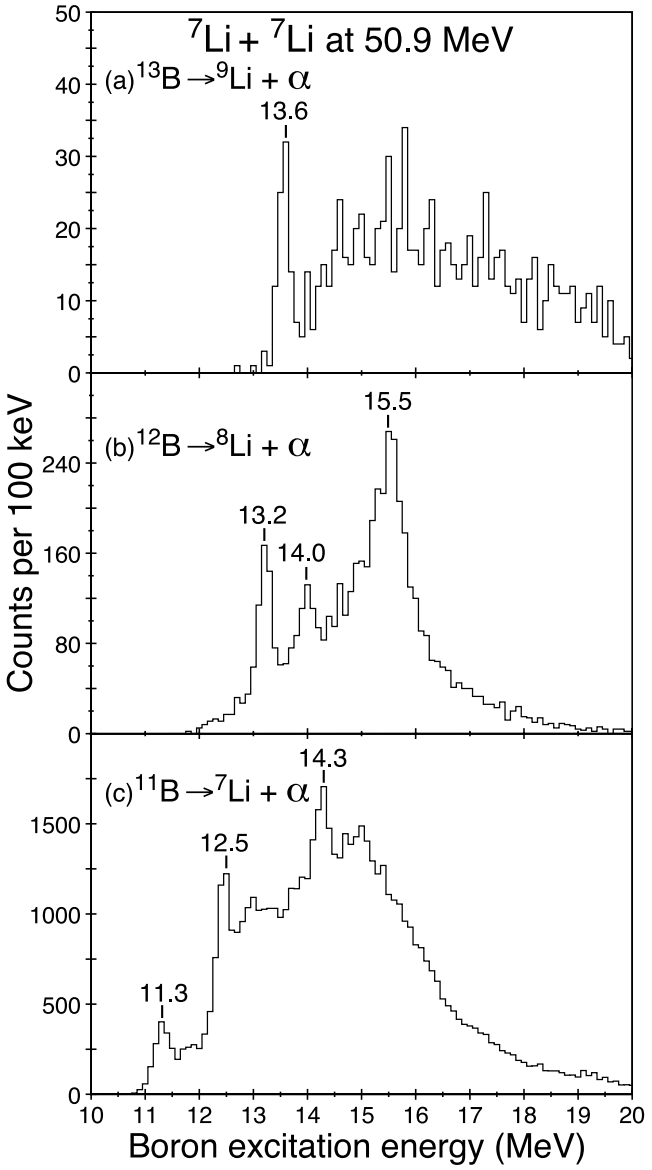

FIG. 5. Direct detection of boron isotope decays into Li(g.s.) $+\alpha$ using the wide angle geometry, $E_A = 50.9$ MeV. Prominent decay energies are labeled. Other possibilities are easily discerned.

states, but poor statistics prevent their substantiation. The states in ^{12}B indicated at 13.2 and 15.5 MeV are probably the known [16] states at 13.33 and 15.5 with 14.0 being a new excitation. The nucleus ^{11}B is well studied [16], and all states indicated in Fig. 5(c) have been previously observed. Some of the yields for B$\rightarrow$Li$+\alpha$ decays seem to be sufficient to pursue an angular correlation analysis as in Ref. [4]; however, the combination of limited data for $\theta(\mathrm{B}^*) \sim 0°$ and the nonzero J values of the $Z=1$ and $Z=3$ decay products would preclude an unambiguous spin determination of the boron excited state.

Coincidences of $\alpha+p$ in the 50.9-MeV data produce excellent resolution in the E_{tot} spectrum, and yield ^{10}Be* decays at $E_x = 22.3$, 24.3, and 25.7 MeV for ^{9}Li (g.s.) decays and $E_x = 26.4$ and 27.3 MeV for ^{9}Li* decays. Coincidences of $\alpha+d$ for the indirect detection of ^{8}Li decays show $E_x(^{10}\mathrm{Be}) = 24.8$, 25.6, 27.0, and 27.5 MeV for ^{8}Li (g.s.) decays and 26.2 and 27.0 MeV for ^{8}Li*(0.98) decays. No useful information comes from $\alpha+t$ coincidence data in spite of good resolution in the E_{tot} spectrum. This channel seems to be dominated by direct breakup of ^{7}Li without the formation of excited states.

At $E_A = 34$ MeV the only case among Li$+\alpha$ coincidences that produces a satisfactory E_{tot} peak is for ^{7}Li and it shows an E_{tot} resolution of about 550 keV. Although ^{7}Li (g.s.) is not completely resolved from ^{7}Li*(0.48), the gate in the higher end of the E_{tot} peak yields evidence for ^{10}Be excitations at 27.2, 27.7, and 28.6 MeV. Gating on the ^{7}Li* region of E_{tot} yields $E_x(^{10}\mathrm{Be}) = 27.2$, 27.8, and 28.6 MeV. All of the $\alpha+(Z=1)E_{tot}$ spectra have resolution of less than 400 keV. For the $\alpha+p$ coincidences we find ^{10}Be*$\rightarrow^9$Li$+p$ decays supporting excitations at 21.7, 22.3, 23.1, and 24.3 MeV. For the $\alpha+d$ segment of this work even though there are several thousand events there is no significant information on ^{10}Be* decays. For the $\alpha+t$ coincidences both the ^{7}Li(g.s.)$+\alpha+t$ events and the ^{7}Li*(0.48)$+\alpha+t$ events are dominated by the direct detection of ^{7}Li*$\rightarrow\alpha+t$ at $E_x(^7\mathrm{Li}) = 4.63$, 6.68, and 7.47 MeV. Because of good statistics in these spectra, we can obtain a width measurement for the 6.68-MeV state of 750–850 keV, depending on the background selection. This is in good agreement with the literature [7] value of $875(^{+200}_{-100})$ keV.

2. Small angle geometry results

Coincidence detection of Li$+\alpha$ produces no real-coincidence three-body final state events, since the remaining $Z=1$ particle cannot carry off sufficient linear momentum perpendicular to the beam axis. For $\alpha+(Z=1$ particle) detection the efficiency for indirect detection of Li-isotope decays of ^{10}Be from the small angle geometry experiment provides data on the decay of high-energy states of ^{10}Be, unlike direct detection for which the geometry has very high efficiency for near threshold decays. Shown in Fig. 6 are the E_{tot} spectra for the three-body final states of ^{8}Li$+\alpha+d$ and ^{7}Li$+\alpha+t$ for coincidences between the light particle pairs. Energy resolution is $\sim$250 keV, providing excellent separation of the final states of ^{8}Li and ^{7}Li. Impurity reactions identified near the high-energy end of these spectra occur because of the carbon and ^{6}Li content in the target and due to gates on the $Z=1$ area of the counter telescope spectrum which included some events from the neighboring mass number. In an E_{tot} spectrum for the ^{9}Li$+\alpha+p$ final state (not shown), a well-defined peak of $\sim$180 counts per channel, occurring at $\approx$29 MeV, is identified as the ground state ^{9}Li events. This peak sits on a background of $\sim$60 counts per channel, which rapidly rises at lower energy, similar to the background increases in Fig. 6 at this energy, obscuring any hope for observing the ^{9}Li excited state at 2.69 MeV. Eighty percent of these ^{9}Li$+p$ decays are found by detecting the α in detector 1 (see lower part of Fig. 1) and the proton in detector 2. This will be designated as $\alpha(1)$, $p(2)$ detection, a notation that will be used through this section. The higher yield for $\alpha(1)$, $p(2)$ detection is likely due to the fact that the resulting ^{10}Be* axis is much closer to the beam

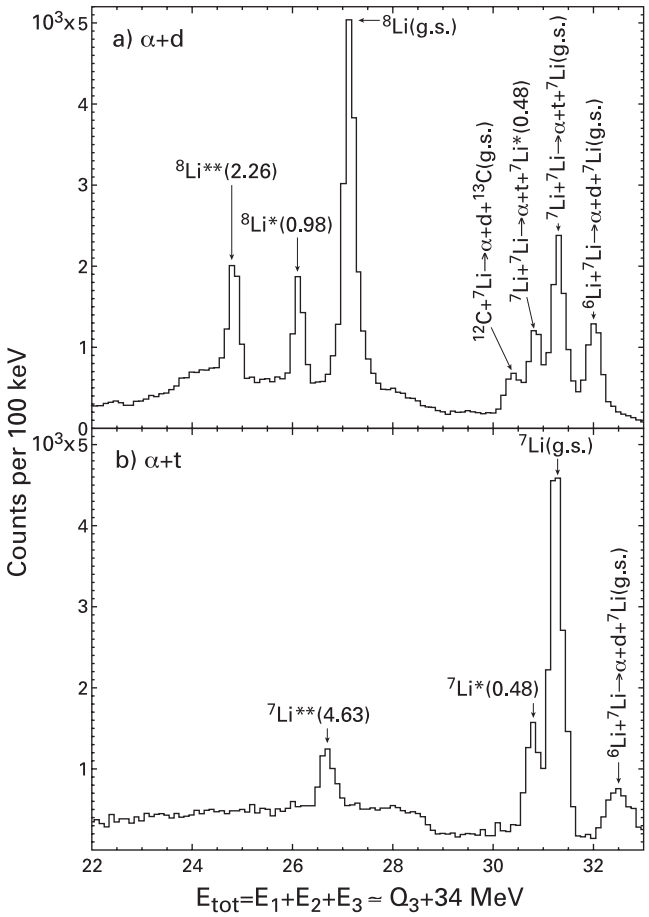

FIG. 6. E_{tot} spectra for (a) $\alpha+d$ detection and (b) $\alpha+t$ detection, using the small angle geometry, $E_{\mathrm{A}}=34$ MeV. Target impurity peaks and those resulting from a generous mass gate on the $Z=1$ portion of the counter telescope spectrum are also labeled.

axis, where yields might be expected to be higher, partly due to kinematic focusing. The ^{10}Be excitation energy spectrum resulting from gating on the ^{9}Li (g.s.) for $\alpha(1)$, $p(2)$ coincidences is shown in Fig. 7. All excitation energies indicated in the figure are substantiated by other observations shown in this paper except for the excitation of 23.0 MeV.

Forming ^{10}Be excitation spectra by gating on the ^{8}Li peaks of Fig. 6(a) is complicated by the fact that the $\alpha+d$ coincidences can also result from the decay of ^{6}Li* in the reaction $^7\mathrm{Li}\,[^7\mathrm{Li},^6\mathrm{Li}^*(2.186\ \mathrm{MeV})\rightarrow\alpha+d]^8\mathrm{Li}$. The problem is illustrated in Fig. 8, which shows Dalitz plots for the $\alpha+d$ coincidence events analyzed as indirect detection of ^{10}Be* decays and as direct detection of ^{6}Li* decays. The locus of points for any particular final state of ^{8}Li forms a near parabolic shape, which moves vertically for different excitations in ^{8}Li and for swapping particle detection between detectors 1 and 2. Since the relative energy between α and d from the first excited state of ^{6}Li remains fixed corresponding to $E_{\mathrm{x}}(^6\mathrm{Li})=2.18$ MeV (horizontal scale), the ^{6}Li* decay events can obscure ^{10}Be* decays over much of the ^{10}Be excitation energy range of 23–30 MeV as the locus of points in the Dalitz plot migrates vertically. A solution to this difficulty is to plot all of the ^{10}Be excitation spectra separately. This is done in Fig. 9 in which several possible excitation energies in ^{10}Be are indicated. In Fig. 9 the yields go off scale at energies where the ^{6}Li* decays interfere. A similarly constructed figure for $\alpha+t$ coincidences, reconstructing excitations in ^{10}Be as $^7\mathrm{Li}+t$ decays, is shown in Fig. 10. Only possible excitations at 22.2, 26.2, and ~27.2 MeV are indicated. An added note of caution: when projecting these Dalitz plots onto the $E_{\mathrm{x}}(^{10}\mathrm{Be})$ axis, even when excited states on the horizontal axis are not possible, the mere shape of the curve (locus of points in the Dalitz plot) may tend to produce broad maxima at the upper and lower energy ends of the

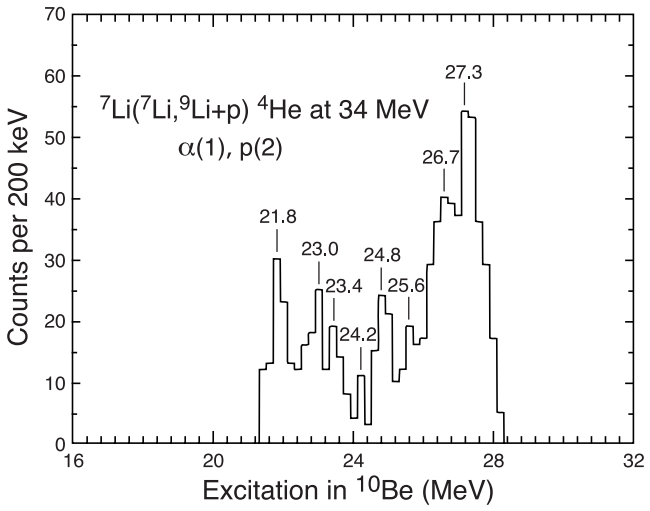

FIG. 7. $E_{\mathrm{x}}(^{10}\mathrm{Be})$ spectrum for $^9\mathrm{Li(g.s.)}+p$ decays indirectly detected, small angle geometry, $E_{\mathrm{A}}=34$ MeV. The notation $\alpha(i)$, $p(j)$ indicates that the α particle is detected in telescope i and the proton is detected in telescope j.

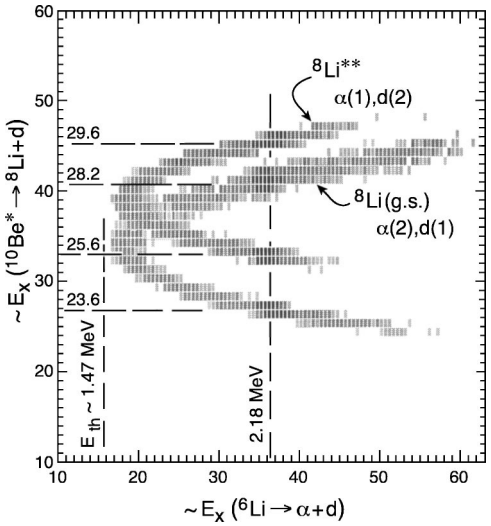

FIG. 8. Two examples of Dalitz plots, $E_{\mathrm{x}}(^{10}\mathrm{Be}^*\rightarrow{}^8\mathrm{Li}+d)$ vs $E_{\mathrm{x}}(^6\mathrm{Li}^*\rightarrow\alpha+d)$ $\alpha+d$ coincidences, small angle geometry, $E_{\mathrm{A}}=34$ MeV. The first excited state of ^{6}Li is detected at ~2.18 MeV, obscuring excitation energy ranges for ^{10}Be* decay. The vertical and horizontal scales for this display are channel numbers with suppressed zeros for their corresponding energy values. For notation see the caption of Fig. 7.

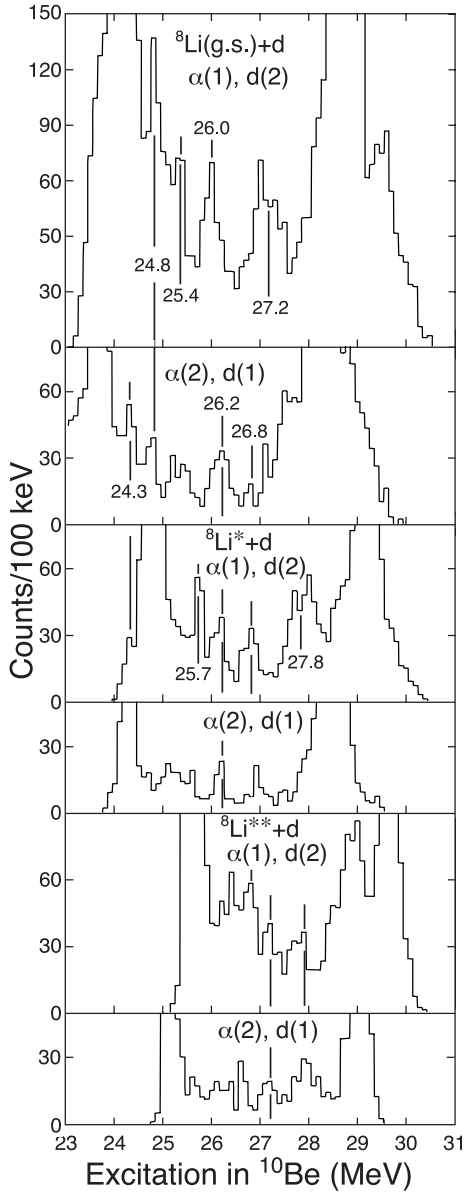

FIG. 9. ^{10}Be excitations from $\alpha+d$ coincidences gated on the ^{8}Li, ^{8}Li*, ^{8}Li** peaks of Fig. 6(a). The off scale yields correspond to decays ^{6}Li*(2.18 MeV)$\rightarrow\alpha+d$. For notation see the caption of Fig. 7.

$E_x(^{10}\mathrm{Be})$ spectrum. These maxima usually are due to changing ^{10}Be* detection efficiency rather than ^{10}Be excitations.

C. ^{10}Be*$\rightarrow^4$He+^{6}He, and ^{4}He+^{6}He*

The direct detection experiments for ^{10}Be decays into ^{4}He+^{6}He have been reported extensively in our earlier work [2,4]. Direct detection of ^{4}He+^{6}He*(1.80 MeV) is not possible by simple means, since the excited state ^{6}He is neutron unstable with an extremely short half-life. Indirect detection of these decays is effected by detecting two α particles and reconstructing the ^{6}He momentum, and hence the relative ^{4}He-^{6}He energy. A typical E_{tot} spectrum for this process is shown in Fig. 11 for the wide angle data at $E_A=34$ MeV.

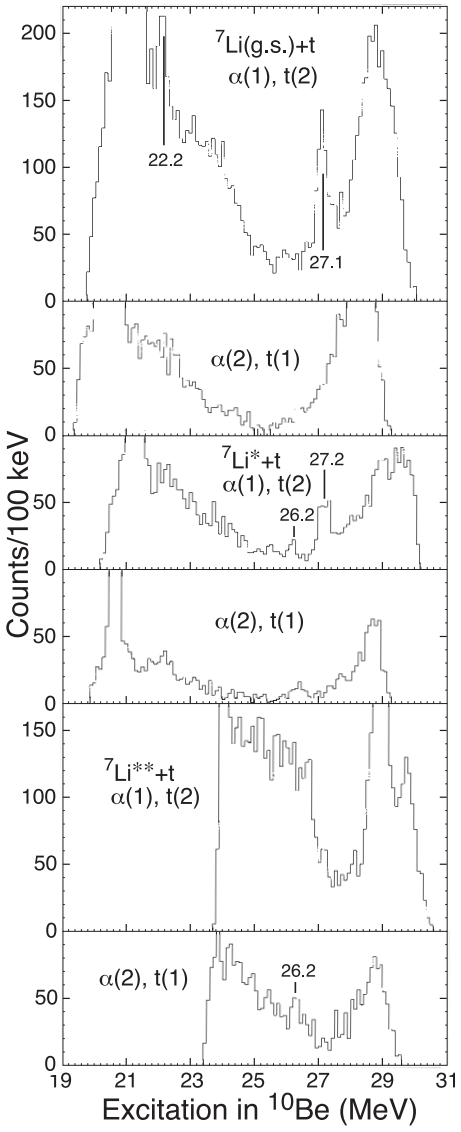

FIG. 10. ^{10}Be excitations from $\alpha+t$ coincidences gated on the ^{7}Li, ^{7}Li*, ^{7}Li** peaks of Fig. 6(b). For notation see the caption of Fig. 7.

The unlabeled peaks are all identified as originating from the ^{12}C content of the target backing with some smaller peaks due to surface oxygen. For $E_A=50.9$ MeV the E_{tot} spectrum is similar, but the yields of interest are reduced by about a factor of 5 and the background continuum has increased. The E_{tot} spectrum for the small angle geometry has been displayed as Fig. 3(a) of Ref. [2].

The wide angle geometry has its maximum coincidence efficiency for a relative energy between the α particles of about 3 MeV, where ^{8}Be has its broad first excited state. For this reason ^{8}Be* detection dominates the spectra reconstructed for ^{10}Be* decay at $E_A=34$ MeV and even more so at 50.9 MeV. We show one such spectrum, Fig. 12, of $E_x(^{10}\mathrm{Be})$ formed by gating on the ^{6}He* peak of Fig. 11. Although the prolific background and statistical considerations make it difficult to unambiguously identify new excitations in ^{10}Be from this spectrum, it is interesting to note several labeled peak energies which are at or near resonances

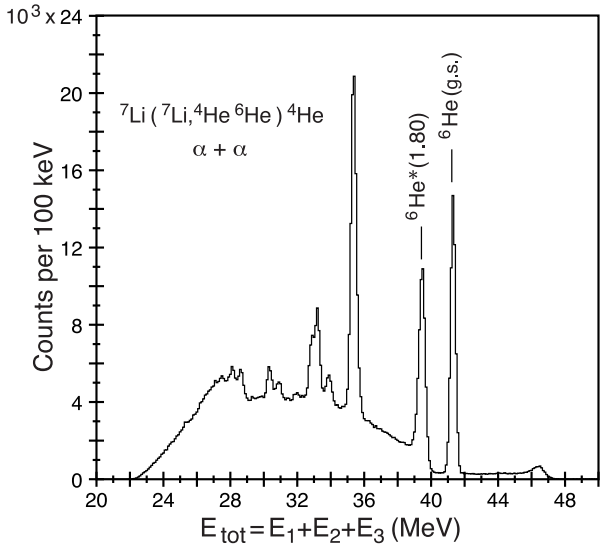

FIG. 11. E_{tot} spectrum for $\alpha+\alpha$ coincidences using the wide angle geometry, $E_{\mathrm{A}}=34$ MeV. The large unlabeled peak is from the reaction $^{12}\mathrm{C}(^{7}\mathrm{Li},^{15}\mathrm{N}^{*}\rightarrow\alpha+^{11}\mathrm{B})\alpha$. Other small peaks correspond to excited states of ^{11}B and reactions on the ^{16}O component in the target.

identified elsewhere in this work. This is the evidence that those states do indeed have a $^{4}\mathrm{He}+^{6}\mathrm{He}^{*}$ decay branch.

The small angle geometry has maximum efficiency for a relative energy between α particles of about 200 keV. This provides very efficient detection of ^{8}Be in the ground state. The energy resolution for the ^{8}Be ground state is ~ 10 keV and it is easily gated out of a spectrum of relative energy

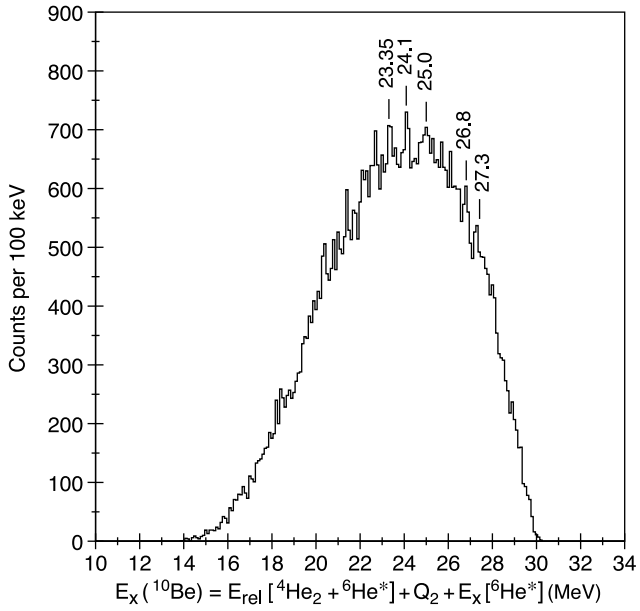

FIG. 12. ^{10}Be excitation energies from $\alpha+\alpha$ coincidences gated on the ^{6}He* peak of Fig. 11, using $\alpha(2)+^{6}\mathrm{He}^{*}$ in the reconstruction, wide angle geometry, $E_{\mathrm{A}}=34$ MeV. All excitation energies labeled are excitations found in the other decay channels from this work. The large background is from the reaction $^{7}\mathrm{Li}(^{7}\mathrm{Li},^{8}\mathrm{Be}^{*})^{6}\mathrm{He}^{*}$.

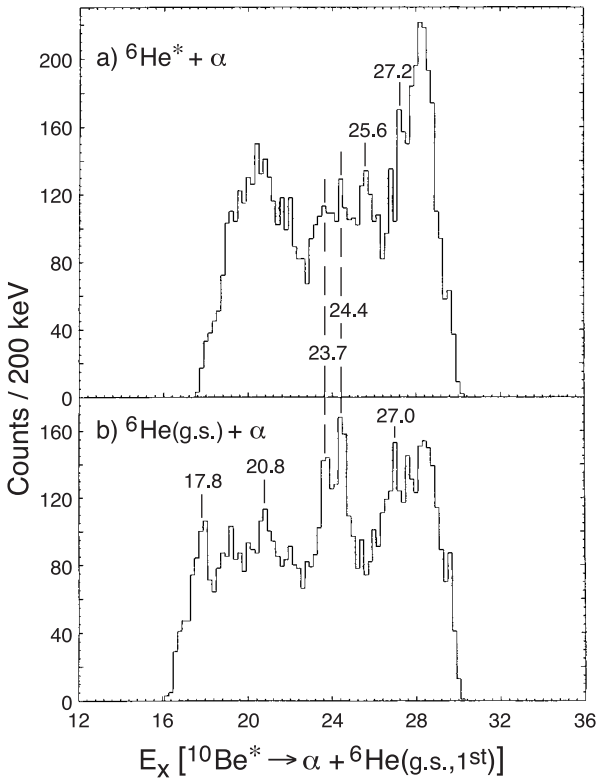

FIG. 13. ^{10}Be excitation energies from $\alpha+\alpha$ coincidences and gates on the ^{6}He and ^{6}He* peaks of an E_{tot} spectrum from the small angle geometry data, $E_{\mathrm{A}}=34$ MeV (see Fig. 2(a), Ref. [2]).

between detected α's. The remainder of α-particle coincidence pairs can be used to reconstruct the $^{4}\mathrm{He}+^{6}\mathrm{He}$ and $^{4}\mathrm{He}+^{6}\mathrm{He}^{*}$ decays of ^{10}Be*. These spectra are shown in Fig. 13. The only new excitation in this spectrum is at 20.8 MeV. All others are also presented elsewhere in this paper.

IV. SUMMARY AND DISCUSSION

In this work we have investigated the charged particle decays of excited states of ^{10}Be in $^{7}\mathrm{Li}+^{7}\mathrm{Li}$ induced reactions at two bombarding energies, using two detector geometries for both direct and indirect reconstructions of the decay, and we have observed ten different decay channels. All of this makes for a very confusing presentation. To summarize the observations, we present Table I in which we identify the figures illustrating each decay branch for all of the excited states observed. Uncertain observations of the excitations are identified by parentheses, and the designation ''nf'' indicates no figure is presented for this observation. Recall that the ''no figure'' designations for the excitations at 19.9 and 21.8 MeV are due to very few events, and those from the triton decays in the 50.9 MeV data are because several different gates on the E_{tot} spectrum were required to determine appropriate excitations. In the left-hand column of the table, the excitation energies listed to the nearest 100 keV have a probable error of 100 keV. Others have a probable error of 50 keV with the exception of the highest excitation. It is likely that the excitation listed at 27.2 MeV is several states from

TABLE I. Summary of evidence from this study for various charged particle decays of ^{10}Be*,( )=uncertain, nf=no figure, see text for details.

E_x(^{10}Be) (MeV)	Figure showing evidence for charged particle decay									
	p	p_1	d	d_1	d_2	t	t_1	t_2	α	α_1
17.8									13	
(19.8)	(nf)									
20.8									13	
21.8	2, 7		(nf)							
22.4	2					10	(10)			
23.0	7									
23.35	7		(3),4			(nf)				12
23.65		2				(nf)			13	13
24.0			3			nf				12
24.25	(7)		3,9	(9)		nf			13	13
24.6		2	3							
24.8	7		3,9	3						
25.05			3	3						12
25.6	(7)			9						13
25.95			3,9	3						
26.3			3,9	3,9			(10)	(10)		
26.8	7		9	9	9					12
27.2±0.2	7		9	3	9	10	10		13	12,13

~27.0 to ~27.4 MeV. Due to limited statistics it is necessary to present some data at 200 keV/channel, which results in peak energies, which do not quite agree with other observations. Many of the excitation energies that are listed in the text do not appear in Table I. Sometimes this is because of the lack of supportive evidence, but often it is because excitations determined for different bombarding energies, detection geometries, or reconstruction techniques can vary by as much as 100 keV. For example, 26.3 MeV appears in Fig. 3 for direct detection of deuteron decay at $E_A=50.9$ MeV, while 26.2 MeV appears in Fig. 9 for indirect detection of deuteron decay at $E_A=34$ MeV, and only the 26.3 MeV value is included in the tables. Excitations above 28 MeV are not included because of the lack of confirming observations.

In Table II we present a comparison of our current results and our previous results from Refs. [2,4], with the 1988 compilation [7] and several other recent experimental works [5,9–13] for excitations below 19 MeV. There is general agreement on the excitations up to 11.8 MeV. It is disturbing, however, that there is not agreement on excitations between 11.8 and the well-known state at 17.79 MeV. Certainly the evidence presented by Bohlen *et al.* [13] for states at 13.6 and 16.9 MeV is convincing. There are four to five excitations reported in the region between 11.8 to 17.3 MeV, without any consistent pattern of agreement amongst three different authors [4,11,13]. Clearly this energy region requires more work. An interesting curiosity occurs for the 18.15-MeV, $J^\pi=0^-$ state found to decay by $t+^7$Li*(0.48 MeV) [2]. In Fig. 8 of Ref. [9] a small anomaly occurs between prominent resonances at 17.79 and 18.55 MeV, at an energy of 18.16 MeV. The authors state that the peak does not possess the proper kinematics for a true resonance; however, such a small effect may be difficult to track. The observed widths of the anomalies are also comparable. From Ref. [2],

TABLE II. Energies and particle decays of unbound states of ^{10}Be($E_x<19$ MeV); comparison of results.

Present work and Refs. [2,4]		Ref. [7]		Ref. [9]		Ref. [5]		Ref. [10]		Ref. [11]		Ref. [12]		Ref. [13]
					Reaction or									
E_x (MeV)	Decay	E_x	Decay	E_x	J^π	E_x	Decay	E_x	Decay	E_x	Decay	E_x	Decay	E_x	Reaction
					^{7}Li(α,p)^{10}Be										^{12}C(^{15}N,^{17}F)^{10}Be
7.542	α	7.542	n	7.542	2^+										
		9.27	n	9.27	(4^-)										
		(9.4)	n			(9.4)	n								
9.56±0.02	α			9.64		9.6	α,n					9.7	α_1	9.55	
10.15±0.02	α			10.2		10.2	α	10.2	α			10.2	α,α_1		
10.57	α	10.57	n	10.57		10.6	α							10.5	
11.23±0.05	α							(11.2)	α						
11.76	α			11.76	(4^+)							~11.8	α,α_1	11.8	
(11.93±0.1)	α									11.9	α				
13.05±0.1	α									13.2	α				
														13.6	
13.85	α														
14.68±0.1	α									14.8	α				
														15.3	
										16.1	α				
				17.12						17.2	α			16.9	
17.79	t,α	17.79	γ, n,t	17.79											
18.15±0.05	t_1			(18.16, see text)											
18.55	t_1	18.55	n,t	18.55											

TABLE III. Energies and particle decays of unbound states of ^{10}Be ($E_x > 19$ MeV); comparison of results.

Present Work		Ref. [7]		Ref. [8]	
E_x (MeV)	Decay	E_x (MeV)	Decay	E_x (MeV)	Reaction or decay
(19.8)	p				
20.8±0.1	α				
		(21.22)	n,p,t	21.207	^{7}Li$(t,p)^9$Li
21.8±0.1	$p,(d)$				
22.4±0.1	$p,t,(t_1)$				
23.0±0.1	p			23.15	^{7}Li$(t,p)^9$Li
23.35±0.05	$p,d,(t),\ \alpha_1$				
23.65±0.05	$p_1,(t),\alpha,\alpha_1$				
24.0±0.1	d,t,α_1	(24)			
24.25±0.05	$(p),d,(d_1),t,\alpha,\alpha_1$				
24.6±0.1	p_1,d				
24.8±0.1	p,d,d_1				
25.05±0.1	d,d_1,α_1				
25.6±0.1	$(p),d_1,\alpha_1$				
25.95±0.05	d,d_1				
26.3±0.1	$d,d_1,(t_1),(t_2)$				
26.8±0.1	p,d,d_1,d_2,α_1				
27.2±0.2	$p,d,d_1,d_2,t,t_1,\alpha,\alpha_1$				

$\Gamma = (100 \pm 30)$ keV, whereas Fig. 8 of Ref. [9] yields $\Gamma \sim 60$ keV. The yield for a $J^\pi = 0^-$ state resonance would be expected to be small because of the large angular momentum mismatch.

The only other comparisons possible between the literature and the present work are presented in Table III. The resonance at $E_x = 23.150$ MeV is observed in the ^{7}Li$(t,p)^9$Li reaction [8], and the tentatively identified state at 24 MeV [7]. We observe a possible expression of the 23.15-MeV state in the proton decay spectrum of Fig. 7, and we observe definite ^{9}Li$+p$ and ^{4}He$+^6$He* decays at $E_x = 24$ MeV. We have no confirmation of the $J^\pi = 2^-$, $T = 2$ resonance at 21.22 MeV [7,8], and such is not expected in these reactions.

V. CONCLUSIONS

The method of RPDS has been shown to be a powerful method for the discovery of charged particle decays of highly excited states in the neutron rich nucleus ^{10}Be. It is particularly useful for finding decays that involve decay products in excited states, since those cannot be observed in resonance reactions even with the use of RIB facilities. We have identified 15 new excitations of the ^{10}Be nucleus in many different decay channels. In these three-body final states, the E_{tot} spectrum has been shown to demonstrate much better energy resolution when particles with smallest Z values are the detected particles. In our case this allowed the $t+\alpha+^7$Li* final state to be clearly resolved [see Fig. 6(b)]. This is probably due to smaller straggling effects when the highest Z particle is left undetected, better intrinsic energy resolution directly proportional to Z^2 [17], and also due to the lack of an energy and angle spread induced by the subsequent γ-ray emission. The improved energy resolution in E_{tot} obtained in indirect detection of decays points to a possible improvement in future experiments.

ACKNOWLEDGMENTS

We would like to thank Powell Barber, Dave Spingler, and the entire graduate student and technical staff for their help in the preparation and data acquisition phases of these experiments. We also thank Dr. D.R. Tilley and Dr. J. Kelley for discussion of the forthcoming $A = 10$ compilation. This work was supported in part by the National Science Foundation under Grant No. 9523974.

[1] N. Itagaki and S. Okabe, Phys. Rev. C **61**, 044306 (2000).
[2] J.A. Liendo, N. Curtis, D.D. Caussyn, N.R. Fletcher, and T. Kurtukian-Nieto, Phys. Rev. C **65**, 034317 (2002).
[3] N. Itagaki (private communication).
[4] N. Curtis, D.D. Caussyn, N.R. Fletcher, F. Marechal, N. Fay, and D. Robson, Phys. Rev. C **64**, 044604 (2001).
[5] N. Soić, S. Blagus, M. Bogovac, S. Fazinić, M. Lattuada, M. Milin, D. Miljanić, D. Rendić, C. Spitaleri, T. Tadić, and M. Zadro, Europhys. Lett. **34**, 7 (1996).
[6] W.D.M. Rae and R.K. Bhomik, Nucl. Phys. **A420**, 320 (1984); R.K. Bhomik and W.D.M. Rae, Phys. Lett. **136B**, 149 (1984); S. Marsh and W.D.M. Rae, *ibid.* **153B**, 21 (1985).
[7] F. Ajzenberg-Selove, Nucl. Phys. **A490**, 1 (1988).
[8] S.N. Abramovich, B.Ya. Guzhovskii, A.V. Ershov, and L.M.

Lazarev, Sov. J. Nucl. Phys. **46**, 269 (1987).
[9] S. Hamada, M. Yasue, S. Kubono, M.H. Tanaka, and R.J. Peterson, Phys. Rev. C **49**, 3192 (1994).
[10] M. Milin *et al.*, Europhys. Lett. **48**, 616 (1999).
[11] M. Freer *et al.*, Phys. Rev. C **63**, 034301 (2001).
[12] D. Miljanic *et al.*, Fiz. B **10**, 235 (2001).
[13] H.G. Bohlen, R. Kalpakchieva, A. Blazevic, B. Gebauer, T.N. Massey, W. von Oertzen, and S. Thummerer, Phys. Rev. C **64**, 024312 (2001).
[14] J. Kelley and D. R. Tilley (private communication).
[15] E. Caurier, P. Navrátil, W.E. Ormand, and J.P. Vary, Phys. Rev. C **66**, 024314 (2001).
[16] F. Ajzenberg-Selove, Nucl. Phys. **A506**, 1 (1990).
[17] C. Lee and N.R. Fletcher, Nucl. Instrum. Methods Phys. Res. A **432**, 313 (1999).